

# High speed outflows driven by the 30 Doradus starburst

M.P. Redman<sup>1</sup>, Z.A. Al-Mostafa<sup>2,3</sup>, J. Meaburn<sup>2</sup> and M. Bryce<sup>2</sup>

<sup>1</sup>*Department of Physics and Astronomy, University College London, Gower Street, London WC1E 6BT, UK*

<sup>2</sup>*Jodrell Bank Observatory, University of Manchester, Macclesfield SK11 9DL, UK*

<sup>3</sup>*King Abdulaziz City for Science and Technology, Astronomy and Geophysics Research Institute, P.O.Box 6086 Riyadh 11442, Saudi Arabia*

2 April 2018

## ABSTRACT

Echelle spectroscopy has been carried out towards a sample region of the halo of the giant H II region 30 Doradus in the Large Magellanic Cloud. This new kinematical data is the amongst the most sensitive yet obtained for this nebula and reveals a wealth of faint, complex high speed features. These are interpreted in terms of localised shells due to individual stellar winds and supernova explosions, and collections of discrete knots of emission that still retain the velocity pattern of the giant shells from which they fragmented. The high speed velocity features may trace the base of the superwind that emanates from the 30 Doradus starburst, distributed around the super star cluster R136.

**Key words:** galaxies:starburst – galaxies:Magellanic Clouds – H II regions – ISM:kinematics and dynamics – ISM:supernova remnants – ISM:individual (30 Doradus)

## 1 INTRODUCTION

The 30 Doradus nebula in the Large Magellanic Cloud (LMC) is the closest example of a giant extragalactic H II region and the largest in the local group of galaxies. It is regarded as undergoing intense enough star formation to be referred to as a ‘mini-starburst’ by Leitherer (1998) and as such is an important nearby laboratory of both massive star formation and starburst phenomena. The highly dynamic nebulosity (e.g. Meaburn 1981; Meaburn 1987) is powered by a super star cluster of  $\sim 100$  massive stars. Remarkable HST imagery of the environment of the central cluster of massive stars has recently been presented by Walborn et al. (2002). The combined winds, UV radiation and supernova explosions from so many massive stars at a similar evolutionary epoch enables the generation of the nested giant (20 – 300 pc diameter) shells that comprise the giant H II region (Meaburn 1980; Meaburn 1990; Leitherer 1998). On the largest scales, surrounding 30 Dor are supergiant (600 – 1400 pc diameter) interstellar shells such as LMC3.

The term ‘shell’ will be used in this paper rather than the commonly used term ‘bubble’ since it is preferable to use a term that is dynamically neutral and constrained to no specific geometry (e.g. spherical). The term ‘bubble’, often erroneously presupposes a roughly spherical, pressure-driven, energy-conserving shell. This is certainly not the case for the supergiant shells which are unlikely to be either spherical or energy-conserving. The division between ‘giant’ and ‘supergiant’ when applied to the LMC shells will be for the diameter ranges above and recently confirmed by the H I observations of Kim et al. (1999). Different, though related,

mechanisms must be involved in the formation of LMC shells in these distinctly separate diameter ranges. The most important difference is that supergiant shells have diameters in excess of the neutral gas scale-height of the LMC.

The overlapping giant shells comprising the halo of 30 Doradus have been shown to be expanding at around  $50 \text{ km s}^{-1}$  (e.g. Meaburn 1984; Chu & Kennicutt 1994) whereas a multitude of 15 pc diameter regions exhibit outflows of  $\gtrsim 200 \text{ km s}^{-1}$ . The latter were interpreted as young supernova remnants in the perimeters of giant shells (Meaburn 1988). Fig. 1 is a cartoon that illustrates the hierarchy of scale sizes present in a giant H II region like 30 Doradus.

The brightest, dominant velocity components of 30 Doradus are complex but seem to be comprised of three distinct velocity regimes corresponding to H I sheets along the sightline. These are at  $250 \text{ km s}^{-1}$ ,  $270 \text{ km s}^{-1}$  and  $300 \text{ km s}^{-1}$  (McGee et al. 1978; Chu & Kennicutt 1994; Kim et al. 1999). In this paper, the systemic velocity,  $V_{\text{sys}}$  is taken to be the average heliocentric velocity ( $V_{\text{HEL}}$ ) of these components,  $270 \text{ km s}^{-1}$ , in agreement with previous observations (see for example Peck et al. 1997; Meaburn 1991; Garay et al. 1993; Clayton 1987).

In this work, the aim is to investigate the faint highest speed phenomena in the halo of 30 Doradus in order to complete the kinematical characterisation of this important giant H II region. New echelle observations of the line profiles of the highest speed phenomena in the halo of 30 Doradus have been made with unprecedented sensitivity. These are described in Section 2. The region of study was in the vicinity of the Wolf-Rayet star R130 and was se-

arXiv:astro-ph/0308213v1 12 Aug 2003

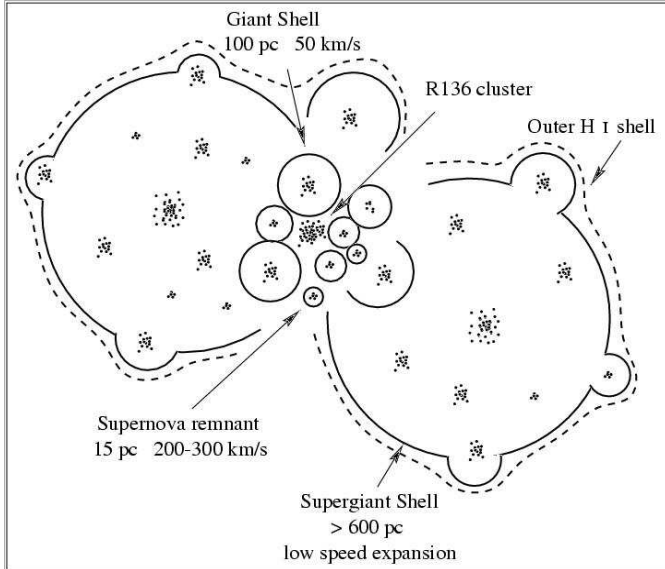


**Figure 1.** Cartoon of the 30 Doradus nebula to illustrate the hierarchy of shell scale sizes. The ambient density increases towards R136.

lected as a representative portion of the halo of 30 Doradus. This area is located in ‘shell 3’, of one of the several giant shells that comprise the 30 Doradus region (nomenclature from Meaburn 1980; Chu & Kennicutt 1994, see also Wang & Helfand 1991) and was one of the regions investigated by Chu & Kennicutt (1994). Section 3 is a discussion of the high-speed motions and morphologies in terms of the structures and dynamics of the giant shells that comprise 30 Doradus. How the high speed features relate to the outflow of hot gas from the 30 Doradus nebula is also discussed. Conclusions are drawn in Section 4.

## 2 OBSERVATIONS AND RESULTS

A reproduction of the ESO PR Photo 14a/02 is shown in Fig. 2. This is an optical image of the 30 Doradus nebula obtained with the Wide Field Imager camera on the 2.2-m MPG/ESO telescope at the La Silla Observatory. A white box marks the region which is investigated spectroscopically in the present work.

Spatially resolved, long-slit echelle spectra of [O III] 5007Å emission lines were obtained using the Manchester Echelle Spectrometer (MES) (Meaburn et al. 1984) at the 3.9M Anglo-Australian Telescope (AAT) on the night of 1994 October 17. The data were obtained using three parallel east-west slits simultaneously, separated by 45'' which were then stepped southwards in 2'' increments. The slit length was 165'' and the slit width was 300 μm ( $\equiv 2''$  and 20 km s<sup>-1</sup>). The broad slit compromises spatial and spectral resolution but permits detection of the faintest, highest speed components of the line profiles. The exposure time for each multi-slit position was 1800s. The locations of all the slit positions are shown in Fig. 3 and the boundary of this figure corresponds to the white box in Fig. 2. In the discussion that follows, a slit is identified by which block of six it appears in. From north to south the blocks are labelled A, B, and C while within a block, also

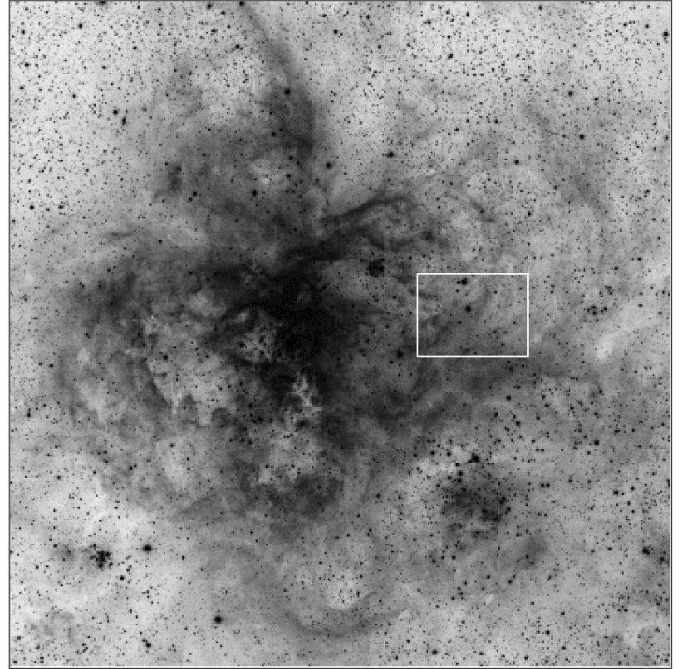


**Figure 2.** 30 Doradus nebula. This figure is a cropped reproduction of ESO PR Photos 14a/02. The white box marks the region from which line profiles were obtained. The size of the region displayed is approximately 200 pc across

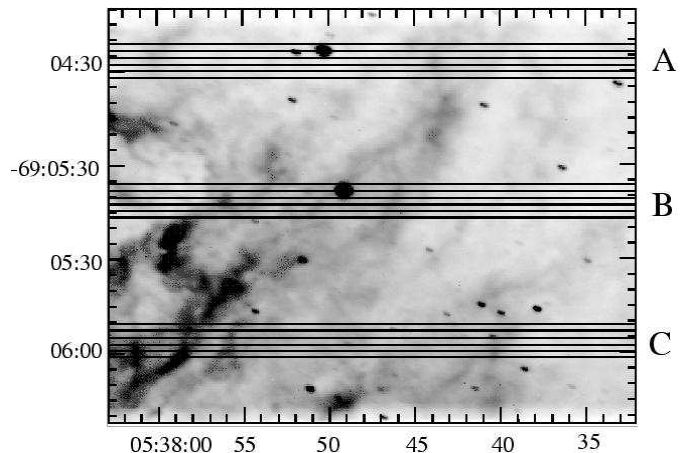


**Figure 3.** MES slit positions marked against the background nebulosity. This region corresponds to the white box in the previous figure

from north to south, the slits are numbered from 1 to 6. The data were processed in the standard manner.

Greyscale representations of the position-velocity (pv) arrays of line profiles obtained from all the slits are displayed in Figs 4–6. These data are also presented and discussed in Al-Mostafa (1999). The scale is logarithmic in these three figures to enable all features to be discerned. In Figs 7 and 8, deep representations of the data from slits C4 and C6 are displayed in order to highlight the faintest, high velocity material.

These data are amongst the most sensitive obtained for the halo of 30 Doradus and reveal a wealth of faint,

complex high speed features. Chu & Kennicutt (1994) carried out echelle spectroscopy across the halo of 30 Doradus but many of the faint, highest speed phenomena revealed here were not detected. In the following discussion, general trends amongst the wealth of complex kinematical features are highlighted. Discussion of individual features may be found in Al-Mostafa (1999). Adopting a distance to the LMC of 55 Kpc gives that  $1'' \approx 0.27$  pc.

### 2.1 Bright systemic features

The pv arrays are dominated by very bright continuous velocity features. These are due to the ionized overlapping H I sheets close to the systemic velocity being disturbed by the slowly expanding ( $50 \text{ km s}^{-1}$ ) giant shells around 30 Doradus (Meaburn 1980; Chu & Kennicutt 1994). These systemic kinematical structures have been investigated in detail in earlier work on the halo of 30 Doradus.

### 2.2 Discrete high speed knots

At the smallest scale (a few arcseconds or approximately one parsec), the pv arrays contain numerous localised high speed ( $\pm 200 \text{ km s}^{-1}$  with respect to the  $V_{\text{sys}}$ ) velocity knots which do not appear to vary widely in spatial scale. They are visible in all the pv arrays and represent the finest-scale high speed substructure detected here.

### 2.3 Velocity loops and arcs

At a slightly larger scale (around ten arcseconds or a few parsecs), individual loops and arcs are discerned. They are not continuous in the pv arrays but are coherent velocity features made up of the discrete velocity knots. The clearest example is that seen at slit position C6 (Fig. 6 and the deep representation, Fig. 8).

### 2.4 Large scale coherent velocity features

At the largest scales (tens of arcseconds or approximately ten parsecs), high speed knots are found to trace out coherent velocity features that slowly vary between being red and blue shifted. The clearest example is perhaps that in slit position B3 where at offsets of approximately 0 to  $50''$  the feature is redshifted and between around 50 and  $100''$  it is blueshifted with respect to the bright continuous feature.

## 3 DISCUSSION

### 3.1 Giant shells in 30 Doradus

The current explanation for the origin of the 30 Doradus nebula is that as the massive stars within the nebula evolve, their winds (especially during the Wolf-Rayet phase) and subsequent supernova explosions generate swept-up shells of ionized gas (Meaburn 1988, 1991). The shells are observed to have a hierarchy of sizes and velocities as one moves further into the halo of 30 Doradus. In the dense centre, the shell sizes and velocities are  $\sim 1$  pc and  $\sim 10 - 50 \text{ km s}^{-1}$  respectively, while in the halo the sizes reach  $\sim 100$  pc with velocities of up to  $100 \text{ km s}^{-1}$  (see Fig. 1). The shells are

prone to instabilities and can break up and fragment, venting the interior pressure. For example a dense shell that is accelerating (due to either a rapid drop in the external density or to a new supernova explosion within the shell) may break up via the Rayleigh-Taylor instability. Alternatively, dynamical overstabilities can also lead to a shell breaking up into fragments (Mac Low & Norman 1993). In both cases, the fragments produced will have sizes of the order of the shell thickness. In general, the halo of 30 Doradus, into which the shells are expanding, is inhomogeneous. This inhomogeneity, and the disruptive effects of nearby supernovae and winds from stars not within the original shell, will mean that a shell will not remain coherent for long.

It is important to note that the LMC is thought to be flattened and viewed close to face-on. The scale height of the H I in the LMC disk was calculated by Kim et al. (1999) to be  $\sim 180$  pc so that it is likely that the structure 30 Doradus may also be somewhat flattened. The scale-height imposes a limit on the sizes of the shells that can be formed, irrespective of how intense and coeval in time the massive star activity is. As the shells grow, they become elongated in the direction of the density scale height (Koo & McKee 1992), leading to a break up of the shell in this direction and a ‘blow-out’ of the hot interior gas into the galactic halo. The remaining structure is known as a galactic chimney (Norman & Ikeuchi 1989) and they have been observed in the Galaxy (Normandeau et al. 1996) and in the starburst galaxy M82 (Wills et al. 1999).

The giant shells of 30 Doradus are likely to be the maximum sized spherical momentum conserving shell structures, since the scale height of the LMC is comparable to their diameters. The supergiant shells far exceed this scale height and may be collections of fossil chimneys viewed face-on and also the result of propagating star formation (see e.g. McCray & Kafatos 1987) that is constrained to proceed in the plane of the galaxy, resulting in a ring shape supergiant shell. The loss of driving pressure means they are expanding in a momentum conserving phase and surround a low density cavity. Such cavities are clearly seen in the H I data of Kim et al. (1999) and Staveley-Smith et al. (2002). The hot gas that has escaped from the interior of the giant shells will enter the LMC halo. There is strong evidence for such a halo in the LMC. (Wakker et al. 1998) have used GHRS/HST observations to detect C IV absorption towards LMC stars that do not reside within a shell. This means the hot gas implied by these observations is not local to the star and is likely to reside in the halo (see also Savage et al. 1997).

### 3.2 Origin of the velocity features

It would seem unlikely that the high speed knots represent random gas clouds within 30 Dor since that would require an explanation for both their hypersonic velocities and the systematic way they are distributed about the pv arrays. In terms of the scenario discussed above (section 3.1), a straight-forward interpretation of the kinematical features is as follows. The largest scale features represent old giant shells that have broken up via Rayleigh-Taylor (RT) instabilities. An instability is generated as the shell is accelerated by its interior pressure through a decreasing ambient density. Those portions of the shell that are expanding in the

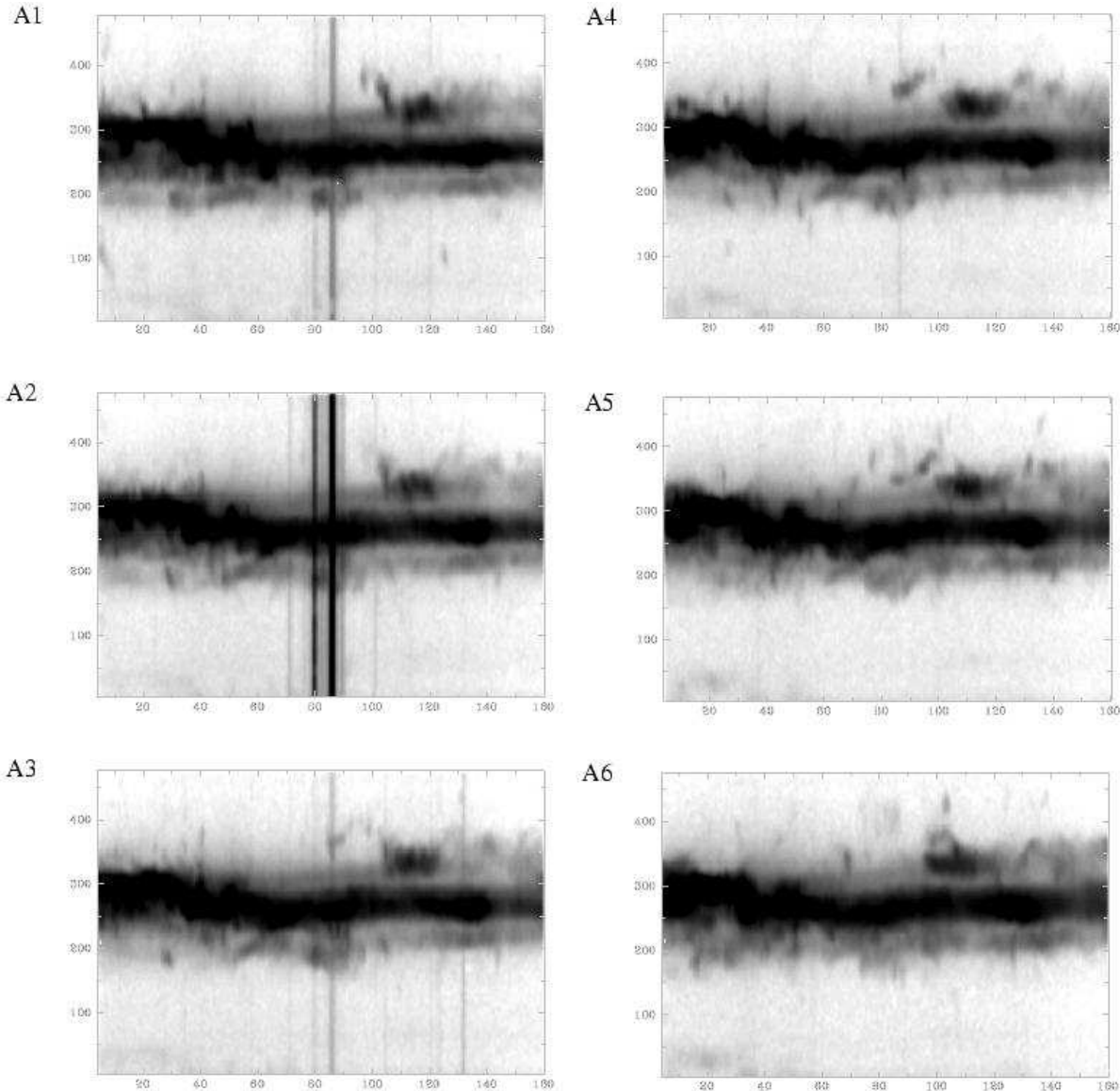


**Figure 4.** Position-velocity arrays of line profiles from slit block A. The vertical scale is heliocentric radial velocity,  $V_{\text{HEL}}$  ( $\text{km s}^{-1}$ ) and the horizontal scale is in arcseconds. At the distance of the LMC,  $1'' = 0.27$  pc.

plane of the LMC are less prone to disruption. The fragments that used to be part of the shell have continued to coast at the pre-break up velocity and together these remain as a coherent velocity feature. For the RT instability, the characteristic knot size at the break up of the shell will be of the order of the thickness of the shell. The sizes implied by this picture seem reasonable - the old shell will have a dimension of up to a hundred parsecs towards the outer regions of the nebulosity while the shell wall will have had a thickness of a few parsecs. These estimates are in accord with measurements of intact shells observed within the halo of 30 Doradus and elsewhere in the LMC (e.g. Oey 1996).

The smaller chains of high-speed knots could be due to more localised disruptions of the giant shells due to, for example, a neighbouring supernova explosion. This latter scenario was proposed by Redman et al. (1999) to explain the unique Honeycomb nebula, which lies in the halo of 30 Doradus. They argued that its cellular structure is due to a

shell that has begun to fragment by a RT instability being impacted by a blast wave from a nearby SN explosion. There have been approximately  $\sim 40$  supernova explosions within the halo of 30 Doradus in the last  $10^4$  yr alone (Meaburn 1991) (in comparison, in the starburst galaxy M82 there have been  $\simeq 50$  SNe in the last  $\simeq 200$  yr; Muxlow et al. 1994).

In the H I pv array data of Staveley-Smith et al. (2002), the LMC and the Galaxy are well separated in velocity. In their data, the Galaxy does not exhibit kinematical features with a  $V_{\text{HEL}} \gtrsim 100 \text{ km s}^{-1}$  while the LMC does not exhibit kinematical features with a  $V_{\text{HEL}} \lesssim 100 \text{ km s}^{-1}$ . In our data faint velocity features are seen from the  $V_{\text{HEL}}$  of 30 Doradus down to a  $V_{\text{HEL}} \lesssim 100 \text{ km s}^{-1}$ . However, it is unlikely that these velocity features are associated with the Galaxy rather than the LMC for several reasons. Firstly, such features are not seen at slit positions offset from 30 Doradus; secondly, many of the features can be traced back

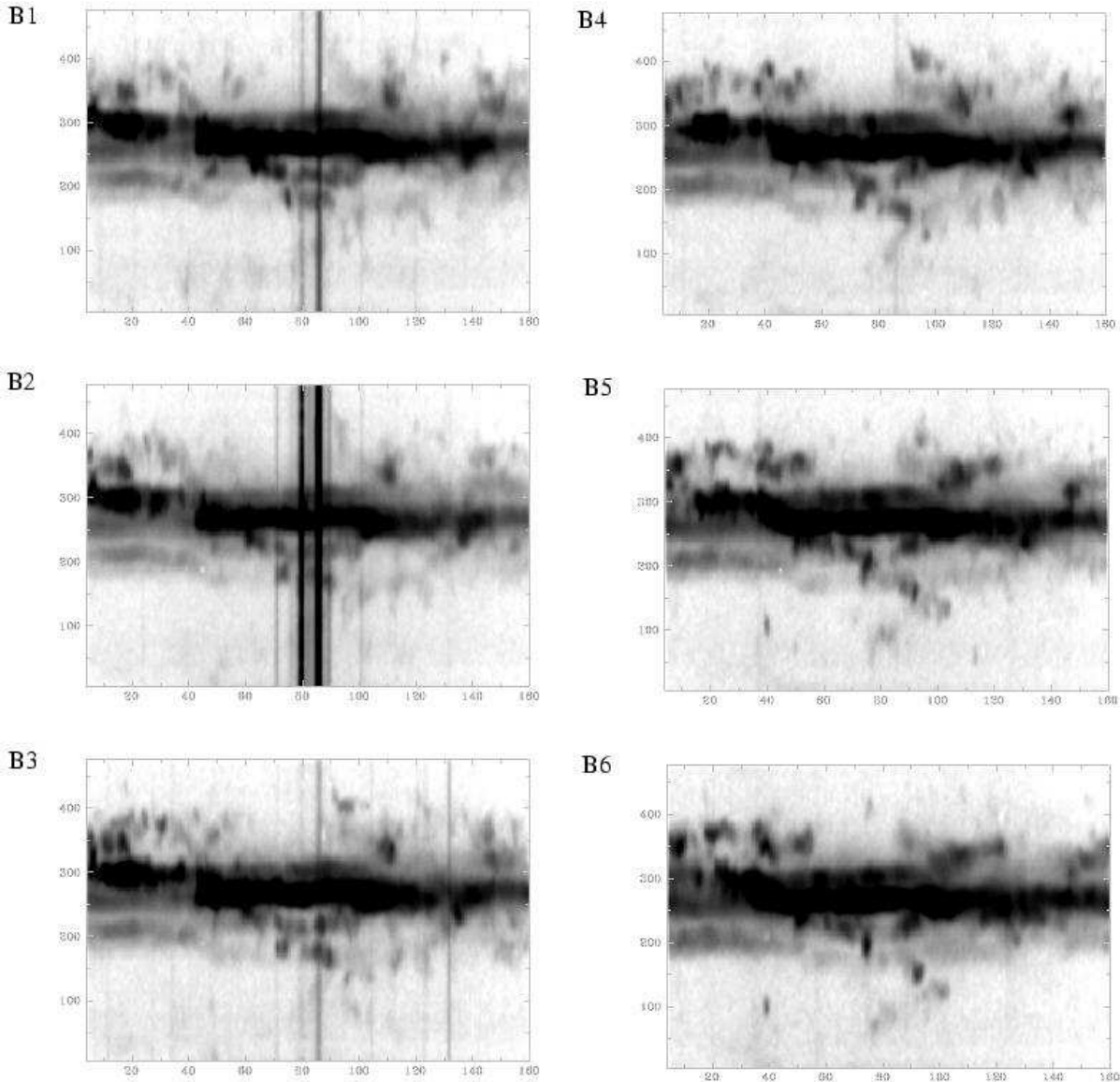


**Figure 5.** Position-velocity arrays of line profiles from slit block B. The vertical scale is  $V_{\text{HEL}}$  ( $\text{km s}^{-1}$ ) and the horizontal scale is in arcseconds. At the distance of the LMC,  $1'' = 0.27 \text{ pc}$ .

to the 30 Doradus systemic velocity; thirdly, there is no known Galactic H II region or ionizing source along the line of sight that could excite the  $[\text{O III}] 5007\text{\AA}$  emitting gas and there is also no extensive background  $[\text{O III}] 5007\text{\AA}$  emission in the galaxy (compare Fig. 7 and 8 here with figure 9 of Staveley-Smith et al. 2002).

### 3.3 Superwind from 30 Doradus

Starburst activity can give rise to a ‘superwind’ due to the intense radiation fields, winds and supernova explosions caused by the star formation. The extensive high velocity features revealed here may be marking the very base of a superwind localised around the 30 Doradus complex. The escape velocity of gas from the LMC in the neighbourhood of 30 Doradus is around  $150 \text{ km s}^{-1}$  so that the high speed ionized gas from disrupted shells and giant shells is escaping

the gravitational pull of 30 Doradus and is being ejected perpendicularly to the plane of the LMC, along the line of sight. The ionization boundary due to the R130 cluster (perpendicular to the plane of the LMC) will depend on the distribution of the gas but an upper limit of a few hundred parsecs can be estimated by calculating the Strömgen radius due to an ionizing flux of  $\sim 10^{51} \text{ s}^{-1}$  from the  $\sim 100$  O stars and a mean gas density of  $\sim 1 \text{ cm}^{-3}$ . Assuming an ejection speed of  $200 \text{ km s}^{-1}$ , it will take of the order  $2 \times 10^6 \text{ yr}$  to reach a distance of  $\sim 500 \text{ pc}$  from the point of origin and thus escape the 30 Doradus region. The gas will rapidly recombine once it has passed the ionization boundary and will then not be visible on the  $[\text{O III}] 5007\text{\AA}$  pv arrays. The dynamical timescale of the remaining giant shell walls is much longer since their progress in the direction of the plane of the LMC is slower than the material ejected perpendicular to the plane. High velocity H I clouds will be formed by the escaping material as it recombines and these clouds

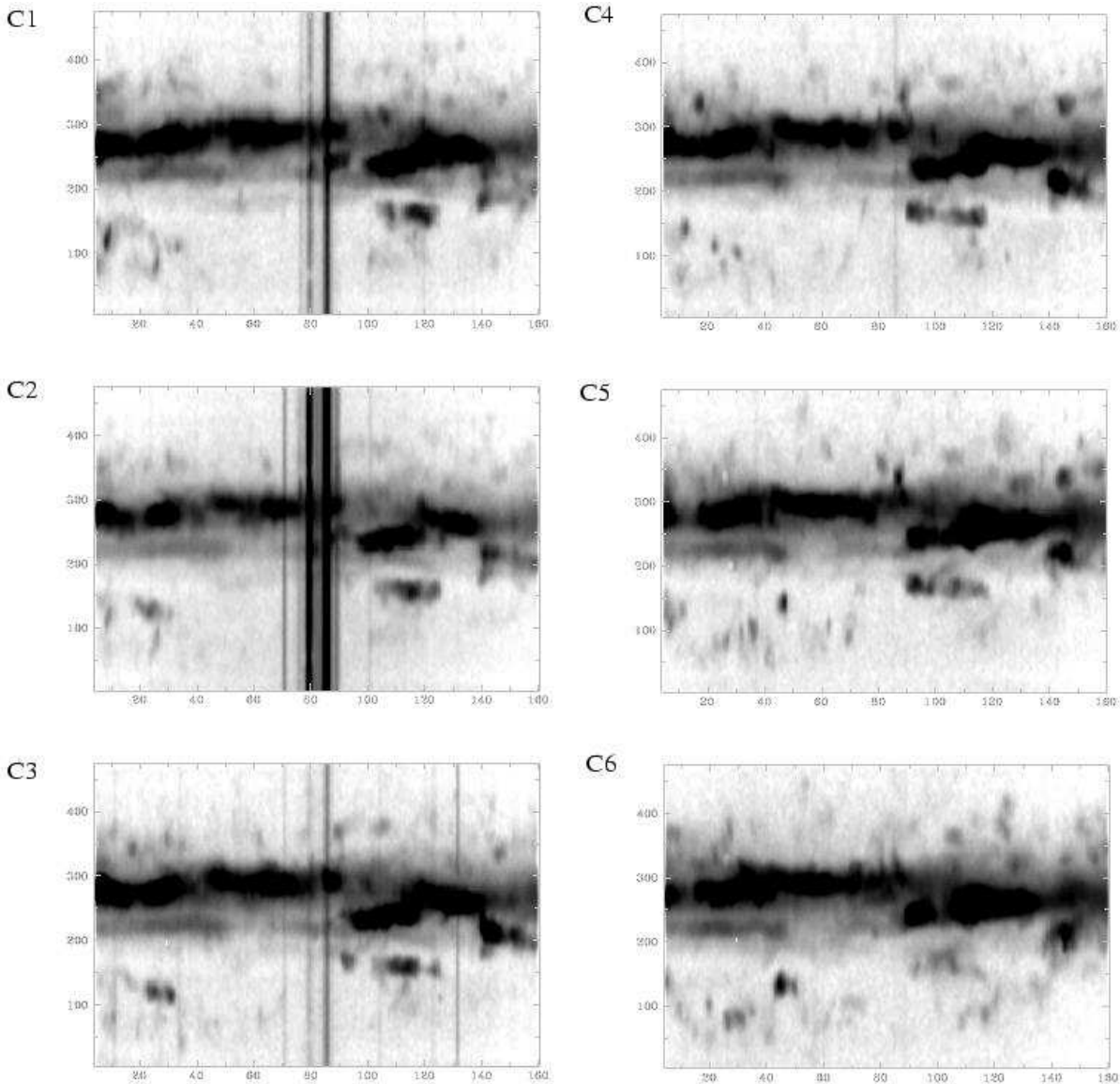


**Figure 6.** Position-velocity arrays of line profiles from slit block C. The vertical scale is  $V_{\text{HEL}}$  ( $\text{km s}^{-1}$ ) and the horizontal scale is in arcseconds. At the distance of the LMC,  $1'' = 0.27 \text{ pc}$ .

may be detectable in high resolution and high sensitivity H I kinematical studies. Of course, the kinematics of gas ejected from the LMC rapidly becomes highly complex due to the interaction with the Galaxy (Wakker & van Woerden 1997).

#### 4 CONCLUSIONS

In this work the kinematics of sample region of the 30 Doradus nebula have been investigated using the MES. This intensive study has revealed high speed velocity features throughout this region. Although the kinematics are complex, general patterns are discerned at three different spatial scales. Small coherent velocity features are present throughout the region. These knots are often found to form loops and chains in the pv arrays and at the largest scales, can form velocity features which vary slowly between red and blue-shifted emission. It is suggested that all of these fea-

tures are explicable in terms of the current understanding of the 30 Doradus nebula. Shells and giant shells formed by the winds and supernovae of massive stars form and are then disrupted in the energetic turbulent environment of the halo of 30 Doradus. The fragments of the shells retain the velocity pattern of the original shell and are observed as the small high speed knots. If this explanation is correct, then high velocity knots are likely to be found across much of the face of 30 Doradus wherever the size of the giant shells have exceeded the scale-height of the LMC and led to ‘blow-out’. The whole 30 Doradus nebula is flattened and viewed face on. The high speed velocity fragments are likely to form the base of an outflowing superwind that is escaping the galaxy. This is a microcosm of the processes that are taking place in starburst galaxies such as M82 in which there are many super star clusters like 30 Doradus and whose combined output lead to the spectacular optical filaments that mark the M82 superwind.

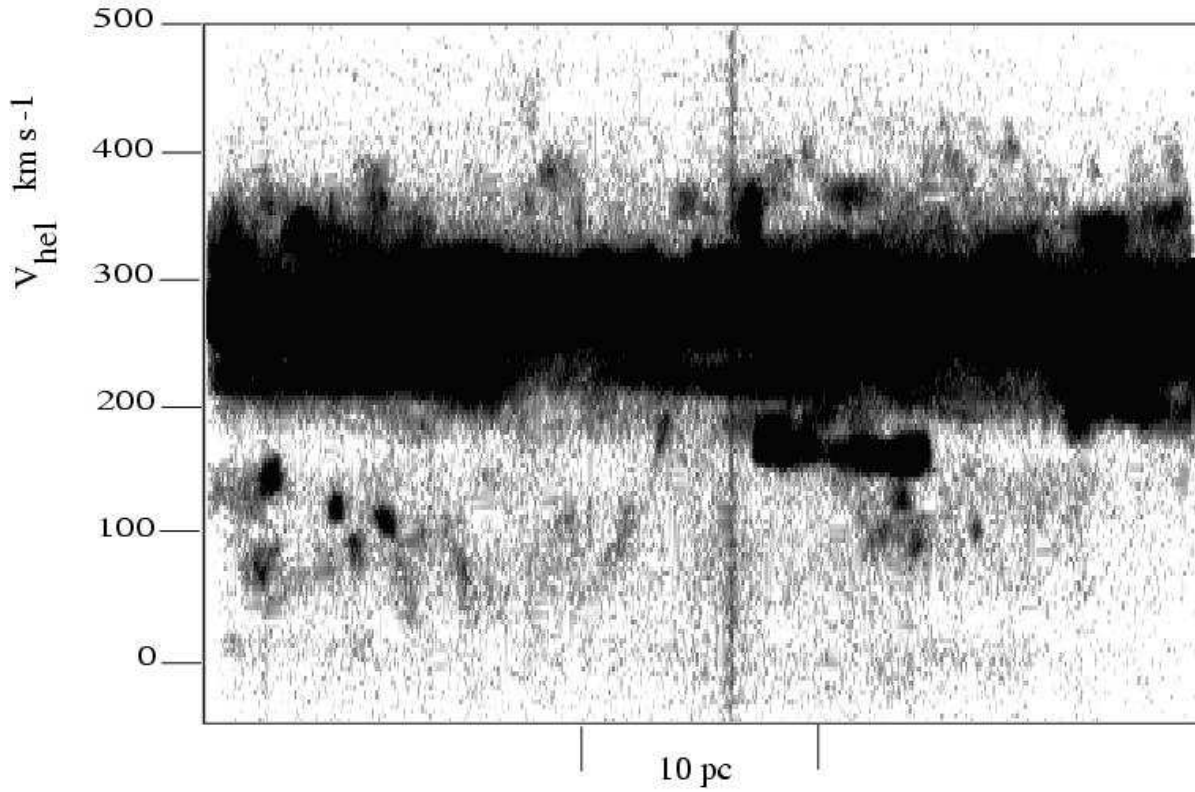


Figure 7. Deep presentation of position-velocity arrays of line profiles from slit block C4 to highlight fainter features.

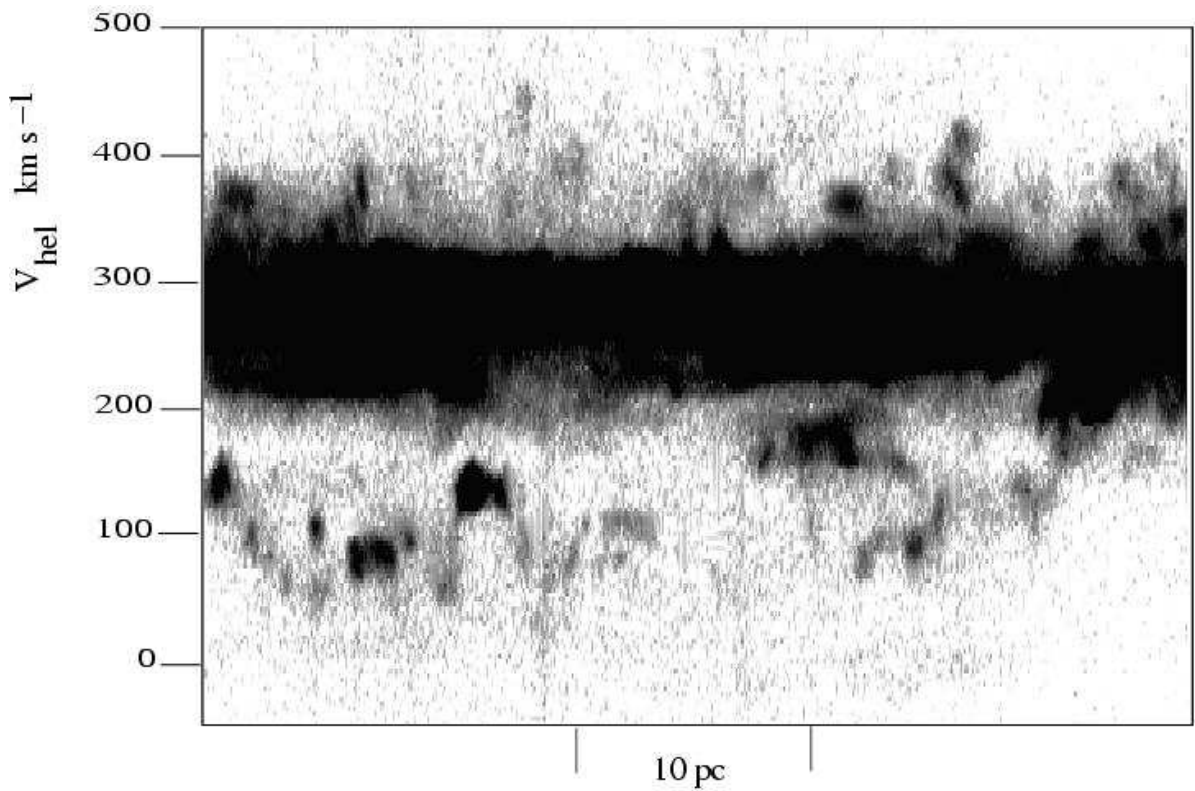


Figure 8. Deep presentation of position-velocity arrays of line profiles from slit position C6 to highlight fainter features.

**ACKNOWLEDGEMENTS**

JM and MB would like to thank the staff at the AAT, who provided their usual excellent service during the observing run. MPR is supported by PPARC. A King Abdulaziz City for Science and Technology ‘KACST’ studentship is acknowledged by ZAA. We thank the referee for comments which improved the paper.

**REFERENCES**

- Al-Mostafa Z. A., 1999, PhD thesis, University of Manchester
- Chu Y. H., Kennicutt R. C., 1994, *ApJ*, 425, 720
- Clayton C. A., 1987, *A&A*, 173, 137
- Garay G., Rodríguez L. F., Moran J. M., Churchwell E., 1993, *ApJ*, 418, 368
- Kim S., Dopita M. A., Staveley-Smith L., Bessell M. S., 1999, *AJ*, 118, 2797
- Koo B. C., McKee C. F., 1992, *ApJ*, 388, 93
- Leitherer C., 1998, in *Stellar astrophysics for the local group: VIII Canary Islands Winter School of Astrophysics Populations of Massive Stars and the Interstellar Medium*. p. 527
- Mac Low M. M., Norman M. L., 1993, *ApJ*, 407, 207
- McCray R., Kafatos M., 1987, *ApJ*, 317, 190
- McGee R. X., Newton L. M., Butler P. W., 1978, *MNRAS*, 183, 799
- Meaburn J., 1980, *MNRAS*, 192, 365
- Meaburn J., 1981, *MNRAS*, 196, 19
- Meaburn J., 1984, *MNRAS*, 211, 521
- Meaburn J., 1987, *MNRAS*, 229, 457
- Meaburn J., 1988, *MNRAS*, 235, 375
- Meaburn J., 1990, *MNRAS*, 244, 551
- Meaburn J., 1991, in Haynes R., Milne D., eds, *IAU Symposium 148 The Magellanic Clouds Studies of the large magellanic cloud using optical interstellar emission lines*. p. 421
- Meaburn J., Blundell B., Carling R., Gregory D. F., Keir D., Wynne C. G., 1984, *MNRAS*, 210, 463
- Muxlow T. W. B., Pedlar A., Wilkinson P. N., Axon D. J., Sanders E. M., de Bruyn A. G., 1994, *MNRAS*, 266, 455
- Norman C. A., Ikeuchi S., 1989, *ApJ*, 345, 372
- Normandeau M., Taylor A. R., Dewdney P. E., 1996, *Nature*, 380, 687
- Oey M. S., 1996, *ApJ*, 467, 666
- Peck A. B., Goss W. M., Dickel H. R., et al 1997, *ApJ*, 486, 107
- Redman M. P., Al-Mostafa Z. A. A., Meaburn J., Bryce M., Dyson J. E., 1999, *A&A*, 345, 943
- Savage B. D., Sembach K. R., Lu L., 1997, *AJ*, 113, 2158
- Staveley-Smith L., Kim S., Calabretta M. R., et al 2002, *MNRAS*, in press
- Wakker B., Howk J. C., Chu Y. H., Bomans D., Points S. D., 1998, *ApJ*, 499, L87
- Wakker B. P., van Woerden H., 1997, *ARA&A*, 35, 217
- Walborn N. R., Maíz-Apellániz J., Bardá R. H., 2002, *AJ*, 124, 1601
- Wang Q., Helfand D. J., 1991, *ApJ*, 370, 541
- Wills K. A., Redman M. P., Muxlow T. W. B., Pedlar A., 1999, *MNRAS*, 309, 395